Autonomous Wide Aperture Cluster for Surveillance (AWACS): Adaptive Sampling and Search Using Predictive Models with Coupled Data Assimilation and Feedback

Dr. Pierre F.J. Lermusiaux
Department of Mechanical Engineering, Center for Ocean Science and Engineering,
Massachusetts Institute of Technology; 5-207B; 77 Mass. Avenue; Cambridge, MA 02139-4307
phone: (617) 324-5172 fax: (617) 324-3451 email: pierrel@mit.edu

Grant Number: N00014-07-1-0501 - FY09
http://mseas.mit.edu/ and http://mseas.mit.edu/Research/AWACS/index.html

LONG-TERM GOALS

This research aims to develop and evaluate new environmental-acoustical adaptive sampling and search methodologies, and improve the modeling of ocean dynamics, for the environments in which the main AWACS experiments will occur, using the re-configurable REMUS cluster and coupled data assimilation.

OBJECTIVES

Specific objectives are to:

i) Evaluate current methods and develop new algorithms for adaptive environmental-acoustical sampling, search and coupled data assimilation techniques (Stage 1), based on a re-configurable REMUS cluster and on idealized and realistic simulations (with NPS/OASIS/Duke)

ii) Research optimal REMUS configurations for the sampling of interactions of the oceanic mesoscale with inertial oscillations, internal tides and boundary layers (with WHOI/NPS/OASIS)

iii) Improve models of (sub)-mesoscale ocean physics and develop new adaptive ocean model parameterizations for specific regional AWACS processes. Study and compare processes and dynamics in these regions (with WHOI)

iv) Provide near real-time fields and uncertainties in AWACS experiments and, in the final 2 years, develop algorithms for coupled physical-acoustical data assimilation among relocatable nested 3D physical and 2D acoustical domains (with NPS)

v) Provide adaptive sampling guidance for array performance and surveillance (Stage 2), and link our MIT research with vehicle models and command and control.

APPROACH

The project is founded on a build-test-build approach, with evaluations at sea. The basic research formulates and tests hypotheses and new methodologies. Idealized and realistic data-driven simulations are utilized. Scientific investigations, development of methods and algorithms, and design of AWACS components are ongoing throughout the program, based on at-sea exercises and post-test analyses.

Report Documentation Page

Form Approved
OMB No. 0704-0188

1. REPORT DATE **2009**	2. REPORT TYPE	3. DATES COVERED **00-00-2009 to 00-00-2009**

4. TITLE AND SUBTITLE **Autonomous Wide Aperture Cluster for Surveillance (AWACS): Adaptive Sampling and Search Using Predictive Models with Coupled Data Assimilation and Feedback**	5a. CONTRACT NUMBER 5b. GRANT NUMBER 5c. PROGRAM ELEMENT NUMBER
6. AUTHOR(S)	5d. PROJECT NUMBER 5e. TASK NUMBER 5f. WORK UNIT NUMBER
7. PERFORMING ORGANIZATION NAME(S) AND ADDRESS(ES) **Massachusetts Institute of Technology,Department of Mechanical Engineering,77 Mass. Avenue,Cambridge,MA,02139-4307**	8. PERFORMING ORGANIZATION REPORT NUMBER
9. SPONSORING/MONITORING AGENCY NAME(S) AND ADDRESS(ES)	10. SPONSOR/MONITOR’S ACRONYM(S) 11. SPONSOR/MONITOR’S REPORT NUMBER(S)

12. DISTRIBUTION/AVAILABILITY STATEMENT
Approved for public release; distribution unlimited

13. SUPPLEMENTARY NOTES

14. ABSTRACT

15. SUBJECT TERMS

16. SECURITY CLASSIFICATION OF:			17. LIMITATION OF ABSTRACT	18. NUMBER OF PAGES	19a. NAME OF RESPONSIBLE PERSON
a. REPORT **unclassified**	b. ABSTRACT **unclassified**	c. THIS PAGE **unclassified**	**Same as Report (SAR)**	**10**	

The technical research involve: (i) develop environmental-acoustical adaptive sampling and search schemes; (ii) evaluate and improve models and parameterizations of (sub)-mesoscale processes, based on model-data comparisons and data assimilation; and (iii) develop new adaptive parameterizations in ocean models. The Error Subspace Statistical Estimation (ESSE) system is employed and improved for coupled data assimilation. For ensemble predictions, it utilizes primitive equation ocean model of our MIT group and the coupled normal-mode acoustic propagation model of the Naval Postgraduate School. During AWACS exercises, (near) real-time environmental field predictions and coupled physical-acoustical adaptive sampling and search recommendations are provided. Algorithms and software for advanced high-resolution physical-acoustical data assimilation (DA) are developed. This involves relocatable nested domains and full feedbacks among sets of nested 3D ocean fields and nested 2D acoustic sections.

The PI and his MIT group are working on collaborative efforts that involve interdisciplinary, multi-scale ocean science and modeling, coupled data assimilation, adaptive sampling and search, adaptive data-driven modeling, multi-model Bayesian estimation, and control theory and optimization. The AWACS research benefits from these other related efforts. Significant components of the AWACS work carried out so far are illustrated in http://mseas.mit.edu/Research/AWACS/index.html.

WORK COMPLETED

Nested Free-Surface Primitive Equation Simulations: New improvements in the coupling of the barotropic mode were implemented in our new free-surface, primitive equation nesting algorithm. In the original algorithm, the vertically integrated right-hand side of the momentum equation was averaged in the fine domain and used to replace corresponding values in the coarse domain. Then the surface elevation and barotropic velocities were computed in the coarse domain and boundary values interpolated for the small domain. This algorithm was chosen to avoid violations to the vertically integrated conservation of mass that can arise in the free surface formulation if the wrong quantities are modified. For the new algorithm, several modifications to the above algorithm were found that also maintained the vertically integrated conservation of mass. First, instead of averaging the vertically integrated right-hand side of the momentum, an intermediate estimate of the barotropic velocity is averaged on the fine grid and used to replace corresponding values on the coarse grid. Second, the surface elevation in the fine grid is averaged and used to replace the corresponding values in the coarse grid. The averaging and replacing of the surface elevation is currently lagged 1 time step behind the transfer of the other variables. Finally the barotropic velocity in the coarse domain at this lagged time step is recomputed to be consistent with the new surface elevation.

Adaptive environmental-acoustic sampling: An OSSE testing adaptive sampling in the context of the SW06-AWACS (Aug.-Sep. 2006) experiment was extended in this fiscal year. A small ensemble of simulations (17) was constructed for two distinctive periods: 24-27 Aug 2006, prior to the passage of tropical storm Ernesto, and 4-7 Sep 2006, after the passage of Ernesto. From these ensembles, four sampling patterns were generated by Kevin Heaney (OASIS) to simulate a fleet of 5 gliders operating for 2 days. The first was a regular grid of the type an experienced oceanographer would generate from knowledge of the topography and typical dynamic structures of the region. The second was a random sampling of possible tracks under the constraint of a given minimum separation of initial positions. The last 2 patterns were generated by a Genetic Algorithm minimizing a cost function representing the uncertainty of the temperature along the sigma-theta=24.7 isosurface before and after the passage of Ernesto. This year the OSSE was continued by generating 6 data sets (3 sampling methods for 2 time

periods) from a simulated true ocean. Each of these data sets was then assimilated into each of the 17 ensemble members over the first 2 days of the simulations (102 simulations in total). On the third simulation day, root mean square (RMS) errors and pattern correlation coefficients (PCC) were calculated for temperature and salinity at three depths (0m-mixed layer; 30m-thermocline; 100m-deep) to evaluate the impacts of assimilating the different sampling schemes.

Model bias estimation: A practical method was researched for non-recursive bias estimation from model-data misfits suitable for computationally large ocean and atmospheric modeling applications and for non-stationary observational networks. We focused on unbiased minimum error variance estimation, without making assumptions on the probability distribution of errors. An issue for recursive bias estimation is related to the fact that updates of the complete error covariance of bias estimates are not practical in full-scale ocean or atmospheric modeling applications. However, without bias error covariance updates, the procedure gives the current batch of data a disproportionally large influence on the bias estimate as compared to the past data. As a result, a bias field then tends to follow the random error component in the data-model misfits. In view of impracticality of Kalman recursions for bias error covariances in ocean modeling, new methods are needed.

Drecourt et al. (2006) have described a non-recursive bias correction scheme for assimilation of altimeter data into an ocean circulation model. The authors resorted to using a Bayesian technique under the assumption of Gaussian error statistics. Such an approach led them to a variational formulation for non-recursive bias estimation that retained full spatial analysis of model-data misfits. However, the developed formalism was suitable only for the cases with fixed data locations and is not as practical when measurements are collected at different spatial locations. We have developed new approaches that treat the measurements as spatially sparse and collected at time-varying spatial locations. One of the methods we followed does not require specification of error covariances. Instead, a smoothness constraint is utilized to replace the filtering role played by error covariances.

Numerical experiments were used to explore the properties and performance of the bias estimation algorithms. For the synthetic data experiments, we used a regional barotropic tidal model described by Logutov and Lermusiaux (2008). In regional ocean modeling, the systematic error can be highly variable in space, with spatial scales dependent on the characteristics of the coastline and bottom topography. We thus chose an area with complex topographic conditions and coastal boundary geometry for our barotropic tidal model test case. A twin modeling experiment was carried out. The true values of the bias were generated by using different model parameters and open boundary conditions (OBCs). Incomplete and noisy measurements of the true model at sparse observation locations were generated and the bias estimation methodology was applied. The estimates of bias were, subsequently, compared against the true bias. Errors in the bias estimates were examined for various numbers of model-data misfit samples and the convergence properties of the procedure were evaluated. A manuscript is being prepared.

Nested high-resolution generalized inverse estimation of barotropic tides: A paper was published describing an inverse scheme for the assimilation of observational data into a depth-integrated spectral shallow water tidal model (Logutov and Lermusiaux, 2008). The inverse scheme is implemented by carrying out an optimization in the OBC space rather than in the data space or model state space.

Published/Completed Work: Burton et al. (2009) discusses a new use of SVD for improved underwater Acoms. Lin et al. (2009) present a method for merging overlapping profile data sets into a single time series of profiles using an EOF fitting technique. In (Wang et al., 2009), we first utilize

data-assimilative environmental and acoustic propagation ensemble modeling to provide input to a scheme that finds parameter values for autonomous sampling behaviors that optimally reduce the forecast of acoustic uncertainty. A second modification of the autonomous sampling behavior parameters occurs in the vehicle in real-time as it samples the ocean. In (Yilmaz et al., 2008), we use Mixed Integer Linear Programming to design sampling tracks which maximize forecast uncertainty along the track. A third paper (Yilmaz and Lermusiaux, 2009) is being finalized.

RESULTS

Nested Free-Surface Primitive Equation Simulations: The modifications to the nesting algorithm improved the coupling of the barotropic mode between the coarse and fine domains. Specifically the changes strengthened the barotropic feed-back from the fine domain to the coarse domain. By averaging the intermediate barotropic velocity instead of the right-hand side of the momentum equation, this feed-back is moved to the latest step in the algorithm before it affects the vertically integrated conservation of mass. The other modifications (feeding back the surface elevation and making a corresponding adjustment to the barotropic velocity) provide fine-to-coarse feed-backs utterly missing from the original algorithm. Figure 1 contains plots of the difference between the barotropic velocity interpolated from the coarse domain with the barotropic velocity from the fine domain. The top row contains the differences from the original algorithm; the bottom row contains the differences from the new algorithm. After only 1 day of simulation, the original algorithm shows synoptic scale differences of 1-4 cm/s over much of the shelf. By the end of the simulation (43 days), the differences have grown to 6-10 cm/s, remain synoptic scaled but cover the whole fine domain. Contrast this with the results from the new algorithm. There is one spot on the southern boundary by the shelfbreak where the differences grow a bit (due to tidal effects). Over the rest of the domain the differences are bounded by 4cm/s and over the vast majority of the domain the differences remain below 1cm/s. The intermediate differences (1-4 cm/s) are largely confined to the shelfbreak and the Hudson canyon, two topographic features whose representations are governed by the grid resolution.

An immediate consequence of the improved nesting was the creation of an improved set of reanalysis fields using this nested configuration (Figure 2). One illustration of this improvement comes from visual comparison to unassimilated mooring data. Figure 3 shows a comparison of meridional velocities from mooring SW30 at 68m to the nearest-neighbor velocities from the reanalyses. On the left is the comparison to the stand-alone 3km resolution fields, on the right is shown the comparison to the nested 1km resolution fields. A bias in the 3km results is absent in the nested 1km results.

Adaptive environmental-acoustic sampling: Using our OSSE for adaptive sampling in the SW06-AWACS region, RMS errors and PCC skill metrics for temperature and salinity are compared for the different sampling schemes (Genetic Algorithm, regular grid, random starting points) in 2 different time periods (24-27 Aug and 4-7 Sep, 2006). Figure 4 shows the RMS errors for the Genetic Algorithm and random sampling schemes relative to the RMS errors for the regular grid sampling scheme. Also displayed in each panel is the average value for each curve. On average, the RMS temperature error for the Genetic Algorithm sampling is 5% better than the regular grid in the August period, 1% better in September. The PCC show similar results with 4% improvement in August and 2% improvement in September. For Salinity the RMS improvements were 8% in August, 5% in September and the PCC improvements were 6% in August, 4% in September. These numbers may seem like small improvements, but they are in fact significant for three reasons: i) the amount of data simulated is small (only a few gliders over 2 days in a large domain); ii) the coast function for the GA does not focus only on ocean predictive skill, but it still leads to improvements; and finally iii), a new

model version usually does not improve skill by much larger numbers (indicating that just a little bit more data well sampled can lead to as significant improvements).

Model bias estimation: To generate minimum error variance bias estimates with no assumptions on the probability distribution of errors, we reduce the bias estimation to quadratic minimization over a set of matrices, with linear constraints. One of the method does not require an inversion in the data space for applications with large amount of observations (satellite or glider data). This bias estimation consists of solving the Helmholtz equation supplied with the model-data misfit values at data locations as Dirichlet boundary conditions and imposing weak smoothness constraint on the bias estimate.

First, twin experiments with our barotropic tidal model were carried out in complex domains. The true tidal bias then has substantial spatial variations. The RMS error of the bias estimate exhibits a significant reduction over the first few (5-10) samples but saturates for larger number of samples. The initial reduction is related to the separation of the random and the systematic error components of the model-data misfits. With only one misfit sample, this separation relies solely on assumptions. With two or more samples, the separation occurs based on model-data misfits, with the role of the prior bias estimate progressively diminishing. For a number of samples up to n= 20-30, the RMS error of the algorithm reduces approximately as $1/\sqrt{n}$. For a larger number of samples, the RMS error saturates if the RMS is estimated over the entire domain but improves if the RMS is estimated at data locations. The RMS error saturates over the entire domain because of the incomplete coverage: bias and random errors are never sampled over portions of the domain and bias errors are not eliminated there.

Model bias estimation from model-data misfits was carried out to identify biases in HOPS simulations for temperature and salinity fields within the framework of the SW06-AWACS experiment held off the coast of New Jersey in 2006. The 3-D biases in HOPS simulations were computed. The biases were found to be attributed predominantly to the initial conditions and most prominent in the shallow areas for both temperature and salinity fields. In addition, numerical diffusion across model sigma surfaces and other numerical effects, most prominent in shallow areas, contribute to the biases.

Nested high-resolution generalized inverse estimation of barotropic tides: A methodology and computational system for forward and inverse regional tidal estimation was presented (Logutov and Lermusiaux, 2008). Test cases in the complex Strait of Juan de Fuca/Hood Canal/Dabob Bay region demonstrated both the quality of the forward solution and the important amplitude & phase corrections provided by the inverse solution. The technique of optimizing the data fit in the open boundary space was found to be somewhat more robust than the method of representers.

Published/Completed Work: In Burton et al. (2009), we present a new scheme based on SVD that creates a communication architecture that optimally pre-distorts the acoustic wave via spatial modulation and detects the acoustic wave with optimal spatial recombination to maximize reliable information throughput. Lin et al. (2009) utilize an EOF method to combine time-varying data profiles from multiple sources into sound speed profiles indicative of conditions at a single site. The resulting profiles have been used in acoustics propagation modeling endeavors and have improved acoustic data-model comparisons. For adaptive sampling, the two-stage approach of Wang et al. (2009) (Figure 5) was shown to be computationally feasible. Daily forecasts of environmental fields and uncertainties were used to generate 10 to 20 scenarios for sound speed sections, which were transferred to acoustic forecasts. Ensembles of acoustic transmission losses and sound speed sections were used to optimize prior estimates for parameters governing “yo-yo” sampling schemes. The summer daily heating was

shown to impact the optimal sampling. In the morning, the optimization chose yo-yo paths to sample the whole water column. In the afternoon, the optimal result was to sample the whole water column on the first trip but to sample the secondary thermocline (afternoon warming) on the return trip. The mixed integer linear programming (MILP) method of Yilmaz et al. (2008) (Figure 6) was shown to solve the optimization problem for path planning using objective functions based on realistic ocean uncertainty forecasts within allotted time limits. The effects of variations on the type of constraints, number of vehicles and time dependence were studied and diverse sensitivity studies carried out. The general framework of the MILP methodology easily incorporates future extensions.

IMPACT/APPLICATIONS

Better modeling of ocean dynamics at sub-mesoscales including tidally-driven processes is required for accurate and useful acoustic predictions. Coupled physical-acoustical data assimilation enhances predictive capabilities and allows for estimation feedbacks including adaptive modeling. Novel environmental-acoustical adaptive sampling is essential for efficient autonomous naval surveillance. Other application areas include coastal seas management, homeland security and geophysical sciences.

TRANSITIONS

Data-assimilative re-analyses for the SW06-AWACS (Aug.-Sep. 2006) were transitioned to Tim Duda (WHOI), John Joseph (NPS) and Arjuna Balasuriya (MIT) for various studies.

RELATED PROJECTS

We collaborate with K.D. Heaney (OASIS) and T.F. Duda (WHOI). Interactions have also occurred with MIT-OE/EAPS (Arjuna Balasuriya) for adaptive sampling and with NPS (John Joseph) for physical-acoustical studies and data assimilation.

PUBLICATIONS

Burton, L.J., A. Puryear, P.F.J. Lermusiaux, and V.W.S. Chan, 2009. Underwater Acoustic Sparse Aperture System Performance: Using Transmitter Channel State Information for Multipath & Interference Rejection, Proceedings of the IEEE Oceans Conference (Bremen, Germany, 10-14 May 2009). [Published, refereed]

Lin, Y.-T., A.E. Newhall, T.F. Duda, P.F. J. Lermusiaux and P.J. Haley, Jr., 2009. Statistical Merging of Data Sources to Estimate Full Water-Column Sound Speed in the New Jersey Shallow Water 2006 Experiment, IEEE Transactions, Journal of Oceanic Engineering. [Submitted, refereed]

Logutov, O.G., 2008. A multigrid methodology for assimilation of measurements into regional tidal models, Ocean Dynamics, 58, 441-460, doi:10.1007/s10236-008-0163-4. [Published, refereed]

Logutov, O.G. and P.F.J. Lermusiaux, 2008. Inverse Barotropic Tidal Estimation for Regional Ocean Applications, Ocean Modelling, 25, 17-34. doi:10.1016/j.ocemod.2008.06.004. [Published, refereed]

Wang, D., P.F.J. Lermusiaux, P.J. Haley, D. Eickstedt, W.G. Leslie and H. Schmidt, 2009. Acoustically Focused Adaptive Sampling and On-board Routing for Marine Rapid Environmental

Assessment, Special issue of the J. of Mar. Sys. on "Coastal Processes: Challenges for Monitoring and Prediction", J.W. Book, M. Orlic and M. Rixen (Guest Eds), DOI: 10.1016/j.jmarsys.2009.01.037. [Published, refereed]

Yilmaz N.K., C. Evangelinos, P.F.J. Lermusiaux and N. Patrikalakis, 2008. Path Planning of Autonomous Underwater Vehicles for Adaptive Sampling Using Mixed Integer Linear Programming, IEEE Transactions, J. O. Eng. 33 (4), 522-537. DOI:10.1109/JOE.2008.2002105. [Published, refereed]

Figures, presentations and other publications are available from: http://mseas.mit.edu/ and http://mseas.mit.edu/Research/AWACS/index.html. All documents are available upon request.

FIGURES

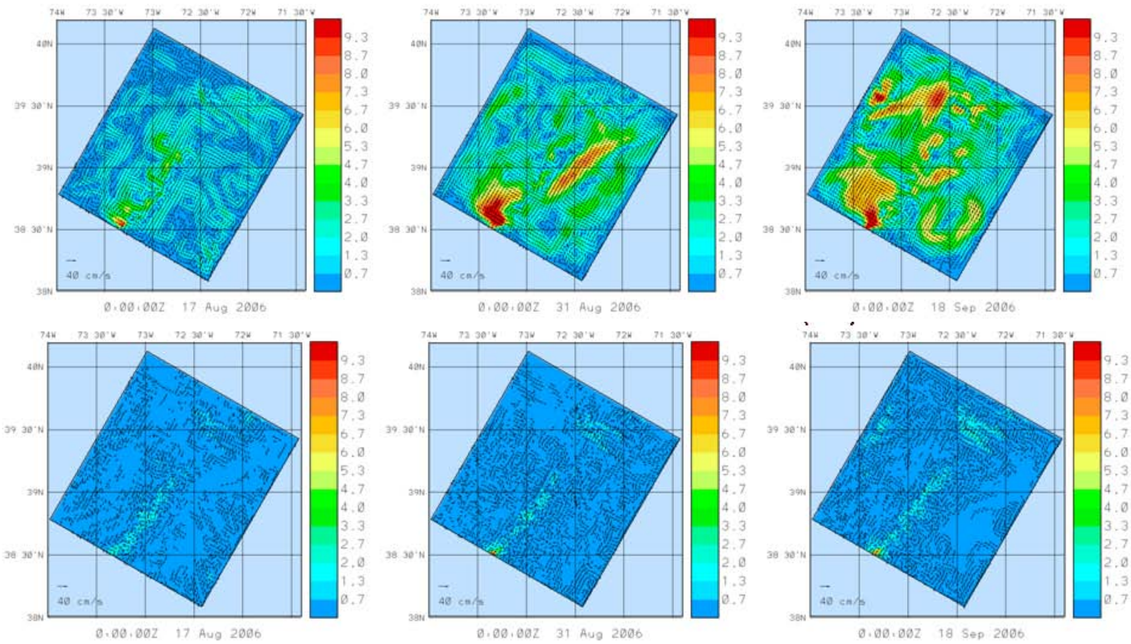

Figure 1. Comparison of drift in barotropic mode for different nesting schemes. Top row, difference in barotropic velocity from coarse domain with barotropic velocity from fine domain for original nesting scheme. Bottom row, same difference but using updated nesting scheme.

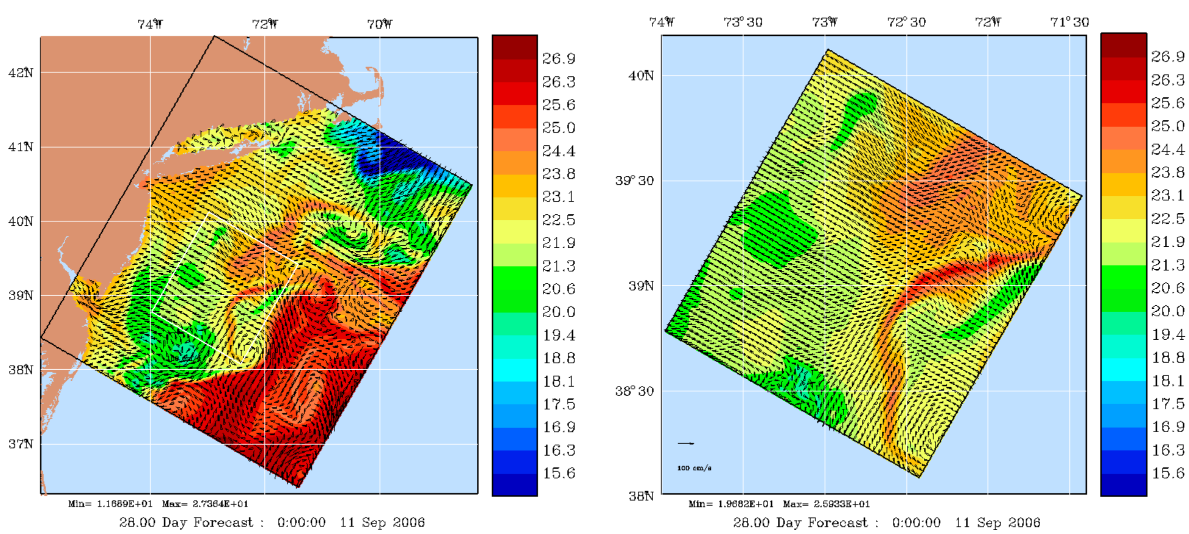

Figure 2. Surface temperature from the new nested reanalysis.

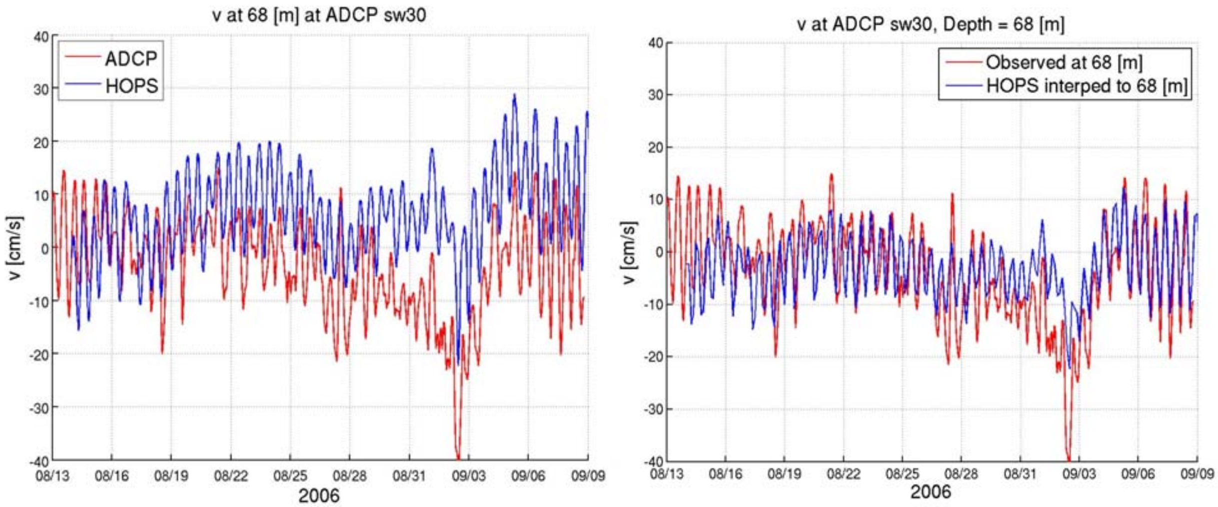

Figure 3. Comparison of mooring meridional velocities to nearest-neighbor velocities from SW06-AWACS re-analyses. Left: stand-alone, 3km resolution reanalysis. Right: new nested 1km reanalysis.

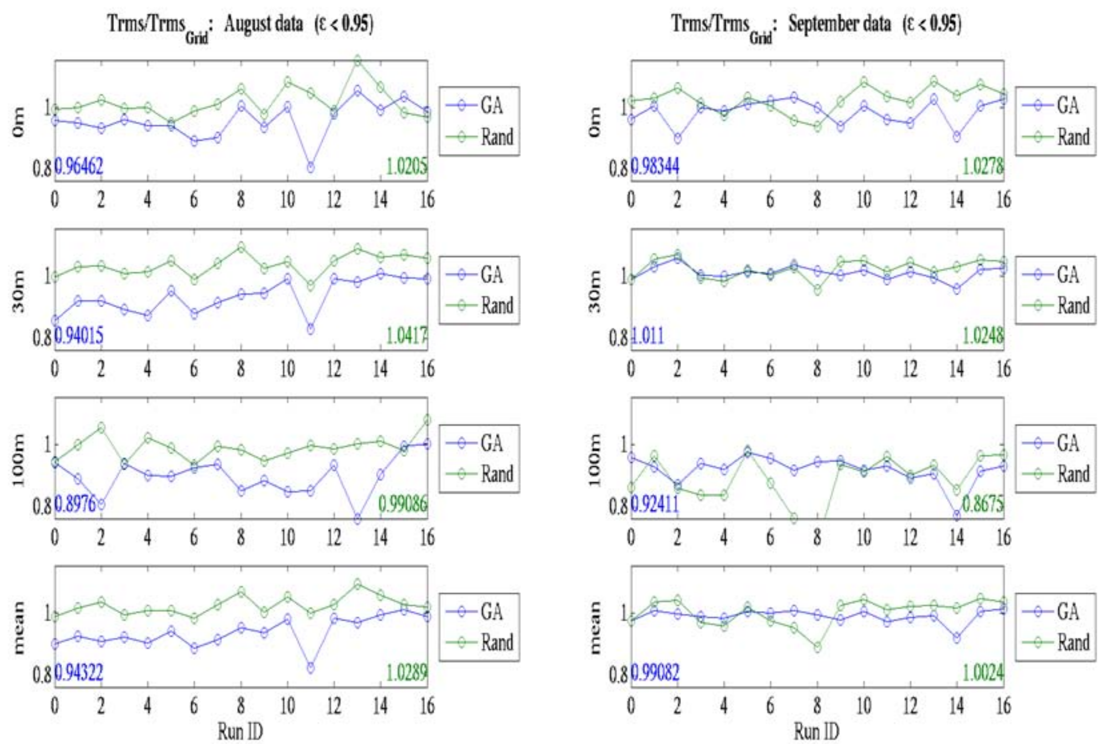

Figure 4. Temperature RMS errors for runs assimilating pseudo-data sampled according to the Genetic Algorithm and random starting points, relative to the temperature RMS errors for runs assimilating pseudo-data sampled on a regular grid. Each panel shows the relative RMS errors for each ensemble member. Also shown in each panel is the numerical value for the average of each curve.

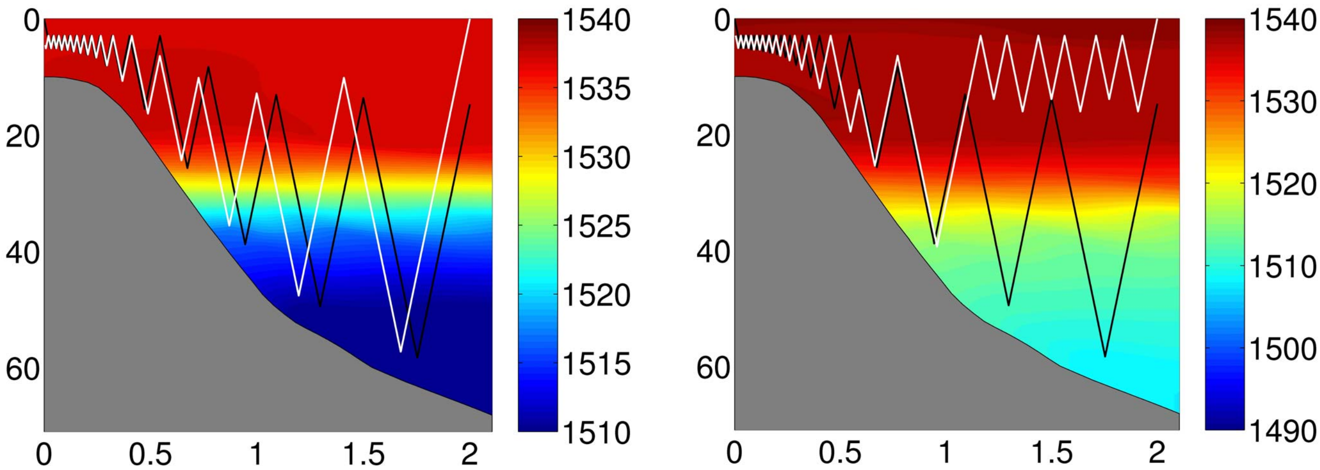

Figure 5. Optimized yo-yo paths for morning (left) and afternoon (right) sampling. Initial path (black) return (white).

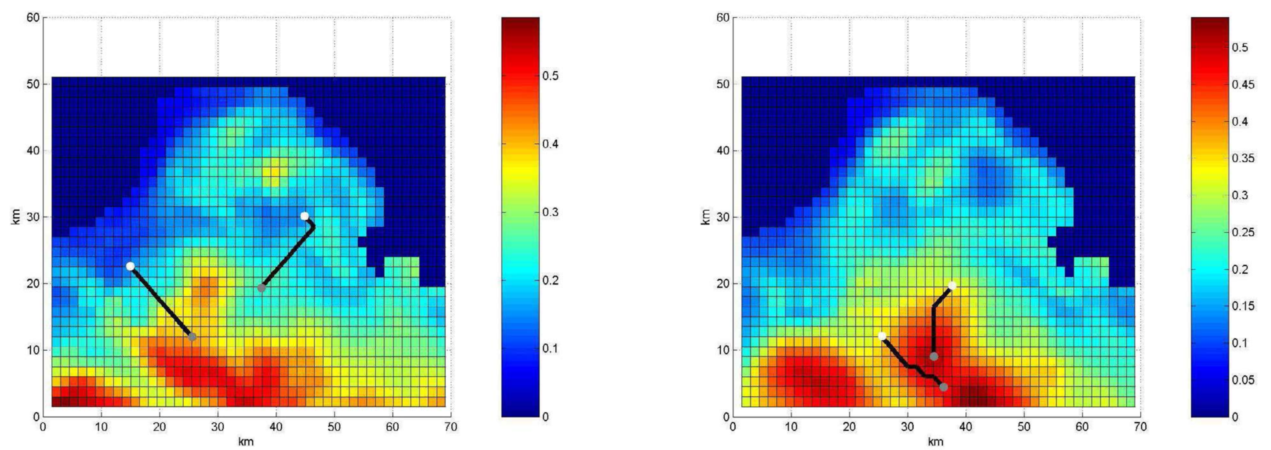

Figure 6. MILP path planning for 2 vehicles with time dependent uncertainty field. Temperature uncertainty fields are shown for day 1 (left) and day 2 (right). Overlain are the sampling paths optimized for the two day for 2 vehicles with each days' starting position in white and terminal position in gray. Note that on day 1, the path on the right samples low uncertainty areas to position the vehicle for sampling very high uncertainty areas on day 2.